

Polycyclic Aromatic Hydrocarbons with armchair edges and the 12.7 μm band.

A. Candian

Leiden Observatory, Niels Bohrweg 2, 2333-CA, Leiden, The Netherlands

`candian@strw.leidenuniv.nl`

and

P. J. Sarre

School of Chemistry, The University of Nottingham, Nottingham, UK

and

A. G. G. M. Tielens

Leiden Observatory, Niels Bohrweg 2, 2333-CA, Leiden, The Netherlands

Received _____; accepted _____

To appear in ApJL

ABSTRACT

In this Letter, we report the results of density functional theory calculations on medium-sized neutral Polycyclic Aromatic Hydrocarbon (PAH) molecules with armchair edges. These PAH molecules possess strong C-H stretching and bending modes around $3 \mu\text{m}$ and in the fingerprint region ($10\text{-}15 \mu\text{m}$), and also strong ring deformation modes around $12.7 \mu\text{m}$. Perusal of the entries in the NASA Ames PAHs Database shows that ring deformation modes of PAHs are common, although generally weak. Therefore, we then propose that armchair PAHs with $N_C > 65$ are responsible for the $12.7 \mu\text{m}$ aromatic infrared band in HII regions and discuss astrophysical implications in the context of the PAH life-cycle.

Subject headings: astrochemistry - infrared: ISM - ISM: lines and bands - ISM: molecules - line: identification - molecular data

1. Introduction

Polycyclic Aromatic Hydrocarbon (PAH) molecules are commonly accepted to be responsible for a family of emission bands, the so-called Aromatic Infrared Bands (AIBs), which are seen in a wealth of astronomical environments: HII regions, photodissociation regions (PDRs), planetary and reflection nebulae, star forming regions, young stellar objects, galactic nuclei and (Ultra) Luminous Infrared Galaxies (Hony et al. 2001; Van Dierendonck et al. 2004; Tielens 2008). However, despite much effort not a single PAH molecule has been identified unequivocally. Understanding the different components of the PAH population in terms of their molecular structure, charge and (de)hydrogenation would allow us to use them as a powerful tool to investigate the physical and chemical properties of astronomical objects (Tielens 2008).

The 11-15 μm region shows a host of features which have been attributed to C-H out-of-plane (OOP) bending modes (Hony et al. 2001). The strongest of these bands peak at 11.2 μm and 12.7 μm and they come together with weaker ones at 11.0, 12.0, 13.5 and 14.2 μm (Hony et al. 2001); all of them are perched upon a featureless and broad plateau (Tielens 2008). The 12.7 μm band, due to the blending with atomic lines ($\text{H}\alpha$ at 12.37 μm , $[\text{NeII}]$ at 12.8 μm) and molecular lines (H_2 0 – 0 S(3) at 12.3 μm) was not studied in much detail before the advent of the Infrared Space Observatory (Kessler et al. 1996). In contrast to the red shaded asymmetric profiles of the 6.2 and 11.2 μm bands, the 12.7 μm band is characterised by a slow blue rise and a red steep side (Hony et al. 2001); its intensity with respect to the nearby 11.2 μm band varies by almost an order of magnitude according to object, reaching its relative maximum in HII regions (Hony et al. 2001). Regardless of their charge, PAHs with duo or trio H show a band near 12.7 μm due to C-H OOP bending modes. As OOP modes are generally weak relative to the CC modes in cations (Hudgins et al. 1994), the 12.7 μm band is

attributed to the OOP modes in neutral molecules containing duo or trio hydrogens (Hony et al. 2001; Bauschlicher et al. 2008; Bauschlicher et al. 2009; Ricca et al. 2012). Here we reexamine the assignment of the 12.7 μm feature based on the results of new quantum chemical calculations.

This Letter is organised as follows: Section 2 contains details of the specific PAH structures studied and the computational methods used; Section 3 discusses the results of the calculations, and in Sections 4 and 5 the astrophysical implications and the conclusions are presented.

2. Computational details

There are several ways to classify PAHs, mostly based on the structure of their carbon skeleton and on the number of adjacent peripheral hydrogen atoms. If we consider PAHs as small sized graphene flakes, they can be divided according to the shape of their edges. Thus we have PAHs with armchair edges like chrysene and PAHs with zigzag edges like tetracene (Figure 1(a)). PAHs with zigzag edges possess mostly solo (non-adjacent) hydrogen atoms, while PAHs with armchair edges possess mostly duo hydrogens which suffer from steric hindrance in the so called bay regions (Figure (1a))

Density functional theory has proven to be a powerful tool to study the vibrational spectra of large molecules such as PAHs (Langhoff 1996; Pathak & Rastogi 2005; Pathak & Rastogi 2007; Bauschlicher et al. 2008; Bauschlicher et al. 2009). In this study, the popular Becke three-parameter (Becke 1993), Lee-Yang-Parr (Lee et al. 1988) B3LYP functional was used in conjunction with the 4-31G basis set (Frisch et al. 1984) on Gaussian 03 (Frisch et al. 2003) to optimize molecular geometries and to compute harmonic vibrational spectra. Langhoff (1996) showed that a scaling factor, 0.958, is needed to

bring theoretical harmonic frequencies into agreement with experimental frequencies; this holds also for PAHs with armchair edges (Langhoff 1996). The spectra are then scaled and convolved with Lorentzian profiles of 30, 20 and 10 cm^{-1} full-width half-maximum (FWHM) in the 3.1-3.4, 6-9, and 9-15 μm regions, respectively. Theoretical IR spectra are in absorption while astronomical IR spectra are in emission; commonly a redshift of 15 cm^{-1} is invoked to account for anharmonicity in the emission process (Bauschlicher et al. 2008). Given the lack of robust constraints on the value of the shift, in this study we chose to be conservative and we do not apply a redshift to the theoretical spectra. The software GABEDIT (Allouche 2010) was used to visualize the results of the calculations, and in particular to view the vibrational modes. The molecular structures studied are summarised in Figure 1(b): they were constructed to have increasing number of bay regions while retaining D_{2h} symmetry.

3. Results & Discussion

The theoretical IR spectra of the studied PAHs between 3 and 15 μm are shown in Fig. 2 (upper and middle rows). They all show strong bands around 3.25 μm and in the fingerprint (11-15 μm) region caused by C-H stretches and bends, as is typical for neutral PAHs (Langhoff 1996). The pyrene-like PAHs (Fig. 2, upper row, first panel) possess several C-H stretching modes resulting in two strong peaks at 3.23 and 3.26 μm , in agreement with previous studies (Bauschlicher et al. 2009; Candian et al. 2012). The major contribution to the first peak is due to the symmetric stretching of C-H bonds involving duo hydrogens, while the second is the result of asymmetric stretching of C-H bonds involving duo hydrogens and trio hydrogens. Increasing the size of the molecule results in more pronounced peaks, with the relative intensity $I_{3.26}/I_{3.23}$ varying from 0.6 to 0.8 and a blue shift of the 3.23 μm peak. Perylene-like PAHs (Figure 2, middle row, first

panel) also possess a double-peaked band in the 3 μm region that behaves similarly.

In pyrene-like PAHs, the 6-9 μm region appears devoid of strong features (Figure 2, upper row, second panel). However, for perylene-like structures (Fig. 2, second row, middle panel) two moderately strong bands occur at ≈ 6.41 and 7.21 μm , the former due to C-C stretching and the latter to a concerted in-plane bending motion of C-H bonds and stretching of C-C bonds. The positions of the bands appear independent of size, while the intensity increases with PAH size as can be expected for the larger number of bonds involved in the mode.

In the fingerprint region (10-15 μm) of pyrene-like PAHs (Figure 2, upper row, third panel) two peaks are noticeable around 12.0 and 12.7 μm . The peak at shorter wavelength is due to C-H OOP bending mode in duo Hs – in agreement with accepted assignments (Allamandola et al. 1989). Visualisation of the atomic displacements proves that the peak at 12.7 μm is the results of two equally strong, almost overlapping transitions due to a duo C-H OOP bending mode and a ring deformation mode (Table 1 and Figure 3). This last vibrational mode is shown as a movie in Figure 3. It involves the rings belonging to the upper part of the armchair structure; the central “lone” rings keep the structure flexible, thus also preserving the intensity of the band for longer molecules. The intensity of the deformation mode increases steadily with number of carbon atoms and/or size as for the C-H OOP mode (Table 1).

In perylene-like molecules (Figure 2, middle row, third panel), the fingerprint region is more complex; the peak around 12.7 μm originates again from the C-C ring deformation mode and the two peaks at ≈ 12.23 μm and ≈ 13.31 μm are due to duo and trio C-H OOP bending modes, respectively. Weak modes present at shorter wavelengths are due to a mix of C-H in plane and C-C bending modes.

The infrared spectra of positively charged $\text{C}_{26}\text{H}_{14}$ and $\text{C}_{30}\text{H}_{16}$ were computed to verify

the effect of ionisation on the ring deformation modes around $12.7 \mu\text{m}$. The band suffers a pronounced decrease in the intensity (Figure 2, lower row, third panel and Table 1), while its position shifts to shorter wavelengths; this is an effect which is generally true for all cationic PAHs compared to their neutral counterparts (Hudgins et al. 1994). Vibrational modes in other regions of the spectrum behave as expected (Figure 2, lower row).

We then inspected the NASA AMES PAH Theoretical Database (Bauschlicher et al. 2010; Boersma et al. 2014) to check whether the ring deformation mode around $12.7 \mu\text{m}$ was present in other neutral and charged PAHs. We found that all PAHs in the database with armchair structure possess a ring deformation mode in the range $12.3\text{-}12.8 \mu\text{m}$. Also PAHs with a non-rigid central ring, such as dicoronylene ($\text{C}_{48}\text{H}_{20}$, uid=100), show a deformation mode around $12.55 \mu\text{m}$. The intensity of the ring deformation mode strongly depends on the flexibility of the carbon structure and on the degree of symmetry. It reaches a maximum in the molecules analysed in this Letter (Figure 1(b)), where the (series) of lone central rings facilitates the ring deformation mode without disrupting the symmetry; a lower symmetry results in decoupling of the vibrational modes. As the carbon structure becomes more rigid, e.g. in the case of $\text{C}_{40}\text{H}_{18}$ (uid=555), the intensity of the deformation mode around $12.59 \mu\text{m}$ rapidly decreases and it becomes very weak in pericondensed PAHs with armchair edges like $\text{C}_{36}\text{H}_{16}$ (uid=128).

4. Astrophysical implications

While the $12.7 \mu\text{m}$ band is seen in a wide range of astronomical environments, it appears to be particularly prominent in the IR spectra of H II regions, where its strength can be comparable to that of the $11.2 \mu\text{m}$ band (Hony et al. 2001). Likewise, the $12.7 \mu\text{m}$ band is very strong in the surface layers of PDRs where the 6.2 and the $7.7 \mu\text{m}$ bands are also (relatively) strong. Our calculations show that neutral PAHs with armchair edges

and/or central flexible ring(s) possess a ring deformation mode in the 12.3-12.7 μm range, where the intensity depends on the flexibility of the molecule and its degree of symmetry. These PAH molecules can thus make an important contribution to the 12.7 μm band strength, especially in H II regions. However, to reproduce the relatively low 11.2/12.7 μm observational intensity ratio, these molecules should not possess solo (non-adjacent) hydrogen atoms. Indeed, the intrinsic intensity of the solo OOP bending mode is higher than the intensity of a ring deformation mode (Candian 2012).¹ Thus, the interstellar 11.2 and 12.7 μm bands must be carried by separate populations of PAHs. In contrast, within this framework, the 12.0 and 12.7 μm bands would result from these armchair PAHs. In Figure 4 we compare the 12.0/12.7 μm ratio as function of size (N_c) in pyrene-like molecules (squares) with the values measured in HII regions (dotted lines) by Hony et al. (2001). This comparison reveals that PAHs in excess of 65 C atoms are needed to reproduce the observed low ratio. This is in agreement with the size estimate for interstellar PAHs derived from the observed 3.3/11.2 μm ratio (Tielens 2008; Ricca et al. 2012).

The observed good correlation between the 12.7 μm band and the 6.2 μm band has always presented an enigma for the PAH model as the former is invariably attributed to neutral PAHs while the latter is carried by ionized PAHs. Generally, this correlation is taken to imply that the conditions that are leading to ionization of interstellar PAHs also promote a high abundance of PAHs with corners (*i.e.*, PAHs with duo and trio H atoms; (Hony et al. 2001; Ricca et al. 2012)). This may then imply that PAHs are rapidly broken down in the ionization zones and the fragmentation process produces small PAHs that carry the 12.7 μm band. However, as the lifetime of small PAHs is expected to be

¹Visualisation of the vibrational modes of dicoronylene with the NASA AMES PAH Database online tool shows a strong (126.1 km/mol) solo OOP bending mode at 11.19 μm , compared to the deformation mode at 12.55 μm (26.3 km/mol).

much shorter than for large PAHs, it is unlikely that this interpretation can withstand a quantitative analysis. Moreover, the main destruction channel for interstellar PAHs is likely initiated by complete dehydrogenation and the formation of pure carbon graphene flakes and/or cages (Ekern et al. 1998; Joblin 2003; Zhen et al 2014; Berné & Tielens 2012). Therefore, breakdown of interstellar PAHs will not favour the formation of the 12.7 μm carriers. The identification of the 12.7 μm band with armchair PAHs proposed here shines new light on this problem. In particular, PAHs with armchair edges are known to be much more stable than PAHs with zigzag edges (Poater et al. 2007). Thus, in the surface layers of PDRs, UV photons lead to rapid ionization while also reducing the interstellar PAH family to its most stable form, the armchair PAHs. Theoretical studies have shown that carbon loss (C_2H_n) from large compact PAHs leads to the formation of armchair structures (Bauschlicher & Ricca 2014). While this class of PAH molecules can describe the qualitative behaviour of the observed 12.7/6.2 μm bands, experimental studies on the photochemical evolution of large PAHs are needed to establish their survival rate and to quantify the abundance of elongated armchair PAH molecules in the ISM.

Candian et al (2012) proposed that the 3.3 μm C-H band of class A – as observed in H II regions – can be explained in terms of a two-component population of PAHs: compact molecules and molecules with bay regions. The PAHs investigated here possess bay regions and show two strong peaks in the C-H stretch region (Figure 3). They can thus contribute to the bay component responsible for the short-wavelength part of the 3.3 μm band. An interesting way to explore this hypothesis would be follow the spatial variation of the two components of the 3.3 μm band and of the 12.7 μm band in a sample of PDRs.

5. Conclusions

In this Letter we studied the vibrational spectra of PAHs with armchair edges by means of Density Functional Theory. The results presented here demonstrate that coupling between the C-H OOP mode and the C-C ring deformation mode in this sub-class of species lead to a strong $12.7 \mu\text{m}$ band. Hence we propose that armchair PAHs with $N_c > 65$ are the main carriers of the interstellar $12.7 \mu\text{m}$ band, previously attributed to duo and trio C-H out-of-plane bending modes. It is inferred that PAHs with armchair edges are favoured in regions exposed to strong UV processing. In the future, the full coverage of the AIB spectrum attained by the *James Webb Space Telescope* will allow us to study the spatial variation of single AIB features with unprecedented sensitivity, helping us to further understand the contribution of PAHs with armchair edges to the astronomical PAH population.

AC acknowledges STFC and The University of Nottingham for scholarships and Cameron Mackie for helping with the animation. Studies of interstellar PAHs at Leiden Observatory are supported through advanced European Research Council Grant 246976 and a Spinoza award. The calculations were performed at the High Performance Computer (HPC) facility at The University of Nottingham (UK) and at the SARA supercomputer center in Amsterdam, The Netherlands (project MP-270-13).

REFERENCES

- Allamandola L. J., Tielens A. G. G. M. & Barker J., 1989, *ApJS*, 71, 733
- Allouche A. R., 2010, *J. Comp. Chem.*, 32, 1
- Bauschlicher C. W. Jr, Peeters E. & Allamandola L. J., 2008, *ApJ*, 678, 316
- Bauschlicher C. W. Jr, Peeters E. & Allamandola L. J., 2009, *ApJ*, 697, 311
- Bauschlicher C. W. Jr et al, 2009, *ApJS*, 189, 341
- Bauschlicher C. W. Jr & Ricca A., 2014, *Theo. Chem. Acc.*, 133, 1479
- Becke A. D., 1993, *J. Chem. Phys.*, 98, 5648
- Berné O. & Tielens A. G. G. M., 2012, *PNAS*, 109, 401
- Boersma C. et al, 2014, *ApJS*, 211, 8
- Candian A., 2012 PhD Thesis, University of Nottingham, UK
- Candian A., Kerr T. H., Song I. -O., McCombie J. & Sarre, P. J., 2012, *MNRAS*, 426, 389
- Cohen M. et al, 1986, *ApJ*, 302, 737
- Ekern S. P., Marshall, A. G., Szczepanski J. & Vala M., *J. Phys. Chem.A*, 102, 3498
- Frisch M. J., Pople J. A. & Binkley J. S., 1984, *J. Phys. Chem.*, 80, 3265
- Frisch M. J. et al 2003, *Gaussian 03*, (Pittsburgh, PA; Gaussian, Inc.)
- Hony S. et al 2001, *A&A*, 370, 1030
- Hudgins D. M., Sandford S. A., & Allamandola L. J., 1994, *Phys. Chem.*, 98, 4243
- Joblin C., in: F. Combes et al. (Eds.) *SF2A – 2003*, *Edp. Sci. Conf. Ser.*, pp.175

Kessler M. F. et al, 1996, *A&A*, 315, L27

Langhoff, S. R. 1996, *J. Phys. Chem.*, 100, 8

Lee C., Yang W., Parr R. G., 1988, *Phys. Rev. B*, 37, 785

Pathak A. & Rastogi S., 2005, *Chem. Phys.*, 313, 133

Pathak A. & Rastogi S., 2007, *Spectrochim. Acta*, 67, 3

Poater J., Visser R., Sol'a M. and Bickelhaupt, F. M., 2007, *J. Org. Chem.*, 72, 1134

Ricca A., Bauschlicher C. W. Jr., Boersma C., Tielens A. G. G. M., Allamandola L. J.,
2012, *ApJ*, 754, 1, 75

Tielens, A. G. G. M., 2008, *ARA&A*, 46, 289

Van Diedenhoven B. et al, 2004, *ApJ*, 611, 928

Zhen J., Paardekooper D. M., Candian A., Linnartz H., Tielens A. G. G. M., 2014, *Chem. Phys. Lett.*, 592, 211

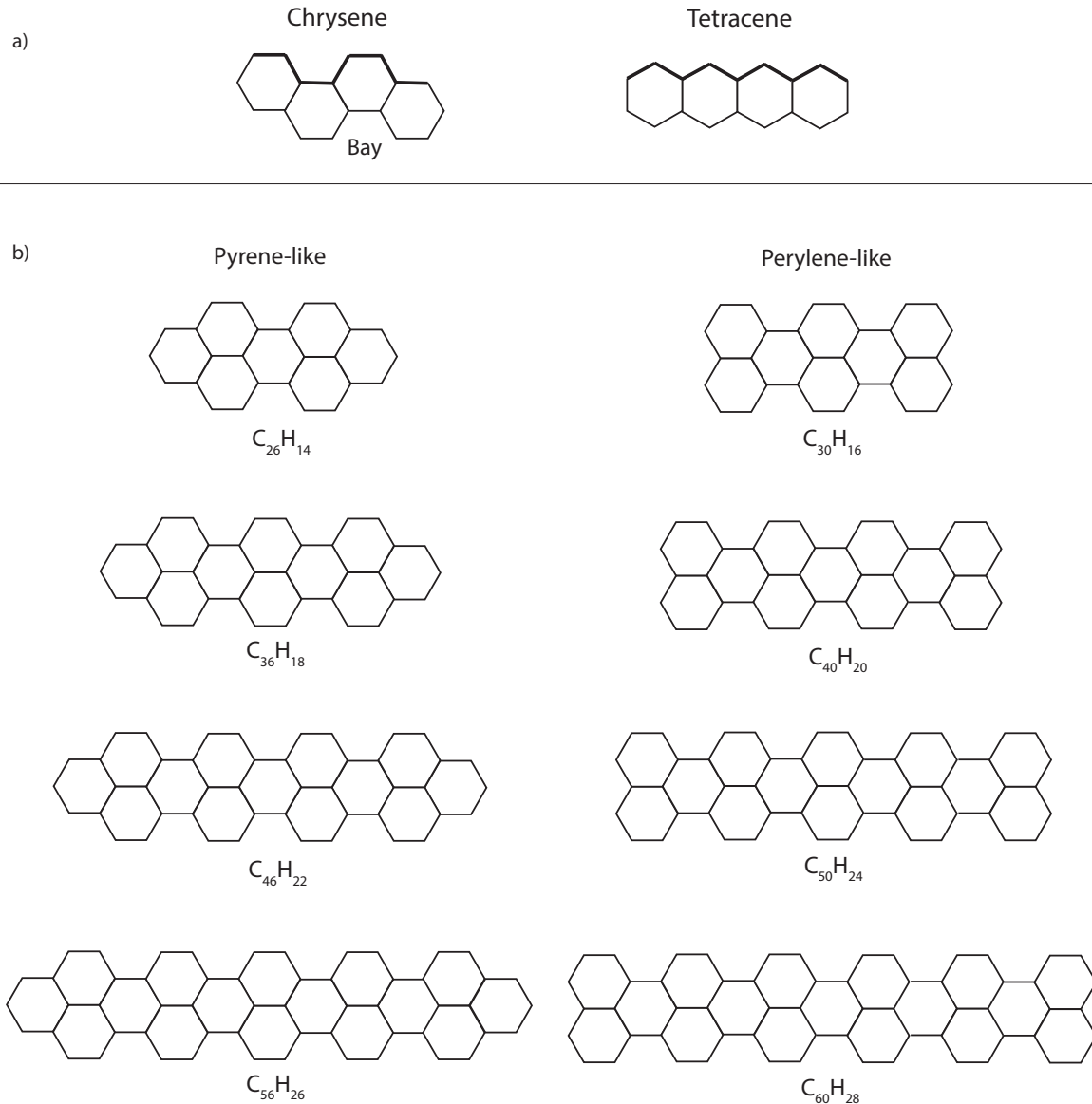


Fig. 1.— (a) Examples of isomeric PAH molecules ($C_{18}H_{12}$) with different edges. Chrysene (left) possesses armchair edges, while tetracene (right) has zigzag edges. Note that PAHs with armchair edges have bay regions. (b) Molecular carbon structures of studied PAHs with armchair edges in order of size. These molecules can be described as pyrene-like (ending with a group of three adjacent hydrogens, *e.g.* $C_{26}H_{14}$) and perylene-like (ending with two groups of three adjacent hydrogens, *e.g.* $C_{30}H_{16}$). All of them belong to the D_{2h} point group.

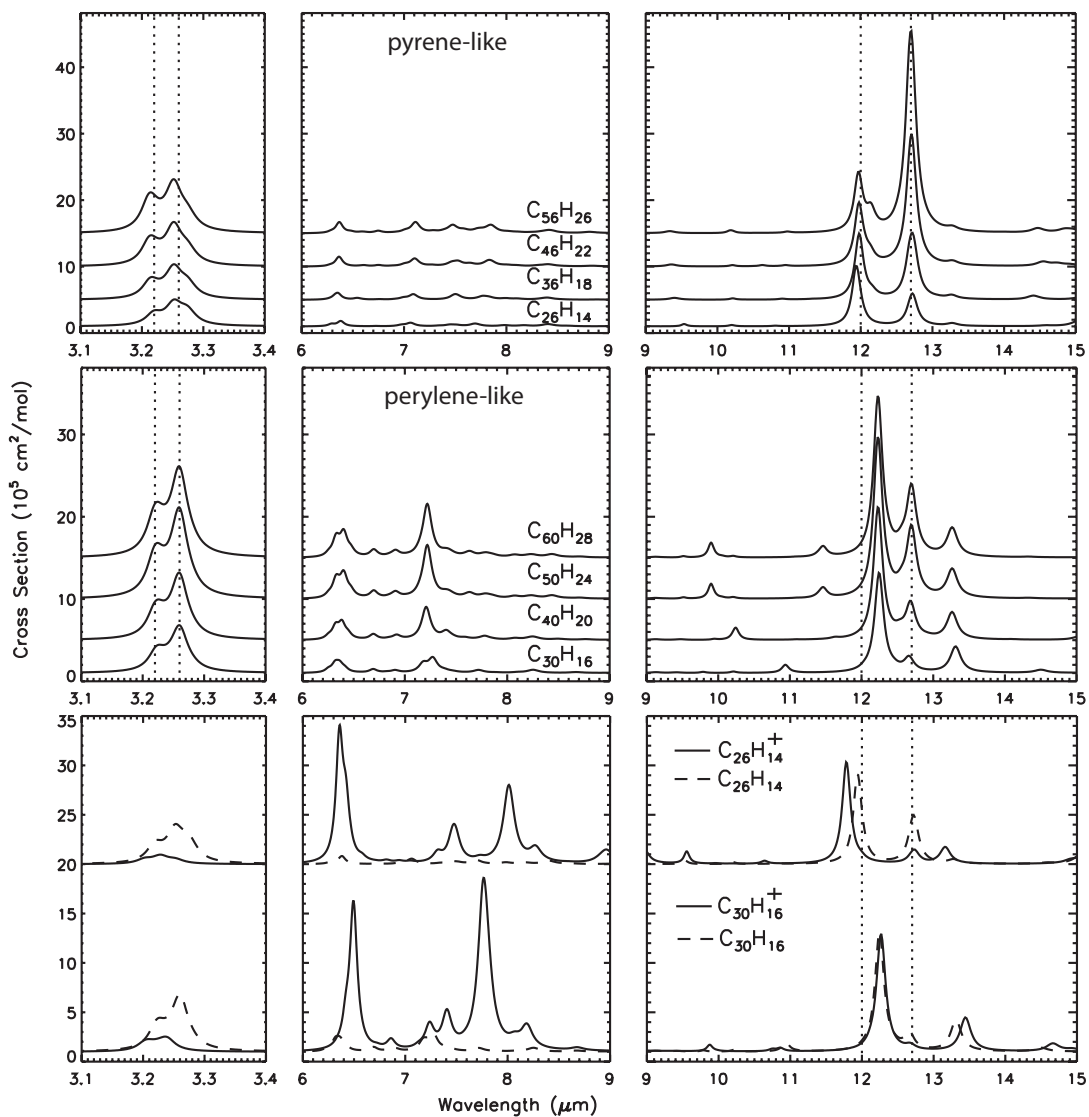


Fig. 2.— Theoretical absorption IR spectra of the molecular structures of Figure 1(b). A Lorentzian broadening and a scaling factor are applied (see text for details). For ease of comparison, dotted lines are drawn at 3.22, 3.26, 12.0 and 12.7 μm . The upper row shows the spectra of pyrene-like structures, the middle row the spectra of perylene-like structures and the lower row a comparison between the IR spectrum of the first member of each series (dashed line), and the spectrum of its positively charged counterpart (solid line).

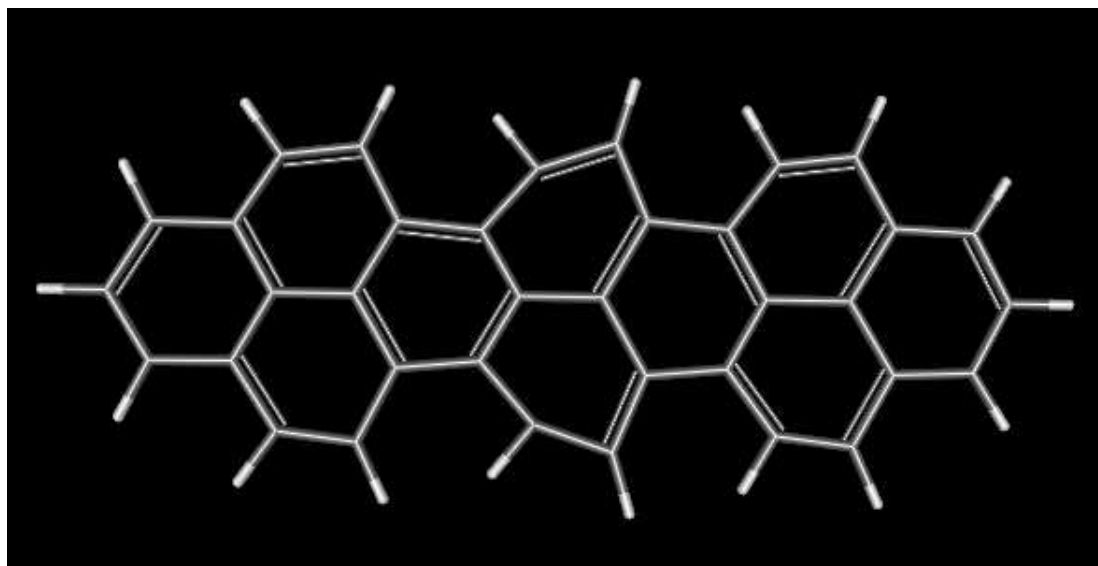


Fig. 3.— Visualisation of the vibrational mode occurring around $12.7 \mu\text{m}$ in $\text{C}_{26}\text{H}_{14}$. The carbon skeleton is shown in grey, the hydrogen atoms in white, and the arrows represent the motion direction and intensity. The ring deformation mode, belonging to the B_{1u} symmetry, involves rings forming the upper part of the armchair edge. (An animation of this figure is available in the online journal.)

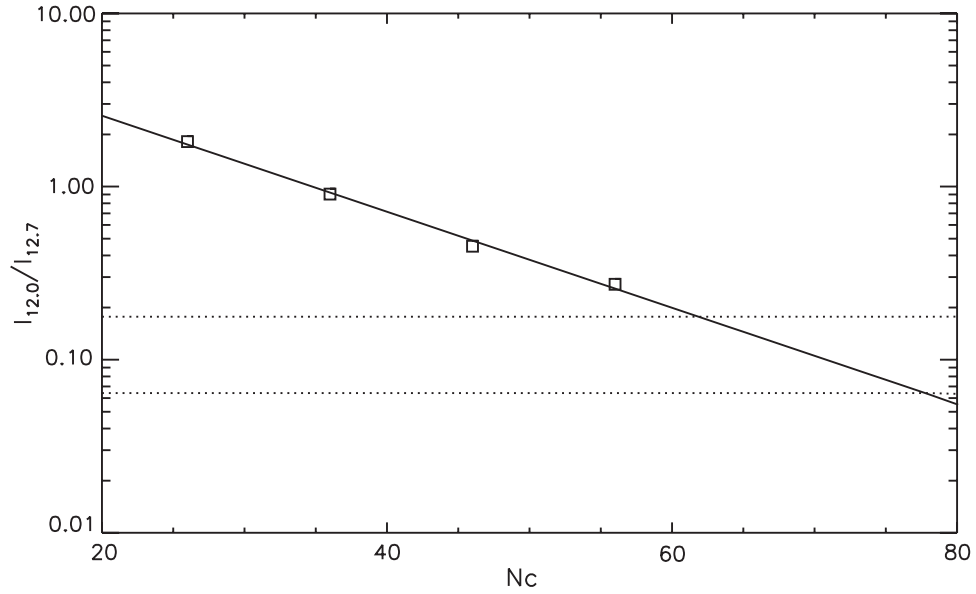


Fig. 4.— Ratio of the theoretical intrinsic intensity of the 12.0 μm band (C-H OOP bends) and the 12.7 μm band (duo C-H OOP bends+ C-C deformation mode) as function of the number of carbon atoms for the pyrene-like series. The solid line shows the result of a linear fit. Calculation of the intensity through an emission model would only slightly increase the ratio given the proximity of the 12.0 and 12.7 μm bands. The horizontal dotted lines indicates the observed astronomical range in HII regions as measured by Hony et al (2001).

Table 1: Vibrational modes in the 12-14 μm Region for the molecules studied

| Pyrene-like | | | | Perylene-like | | | |
|---------------------------------|------------------------------------|-------|------|---------------------------------|------------------------------------|-------|------|
| Molecule | μm (cm^{-1}) | Int | Type | Molecule | μm (cm^{-1}) | Int | Type |
| $\text{C}_{26} \text{H}_{14}$ | 11.93 (837.6) | 140.9 | C-H | $\text{C}_{30} \text{H}_{16}$ | 12.25 (816.6) | 190.3 | C-H |
| | 12.71 (787.0) | 23.1 | C-C | | 12.66 (789.8) | 25.3 | C-C |
| | 12.72 (785.8) | 54.4 | C-H | | 13.31 (751.2) | 49.4 | C-H |
| $\text{C}_{36} \text{H}_{18}$ | 12.00 (834.9) | 153.5 | C-H | $\text{C}_{40} \text{H}_{20}$ | 12.23 (817.6) | 246.2 | C-H |
| | 12.67 (788.1) | 73.0 | C-C | | 12.68 (788.4) | 64.8 | C-C |
| | 12.74 (785.2) | 96.7 | C-H | | 13.26 (754.0) | 50.7 | C-H |
| $\text{C}_{46} \text{H}_{22}$ | 11.97 (835.2) | 141.3 | C-H | $\text{C}_{50} \text{H}_{24}$ | 12.23 (817.7) | 304.5 | C-H |
| | 12.70 (787.2) | 148.0 | C-H | | 12.70 (787.6) | 129.2 | C-C |
| | 12.71 (786.7) | 164.6 | C-C | | 13.26 (753.9) | 52.9 | C-H |
| $\text{C}_{56} \text{H}_{26}$ | 11.97 (835.6) | 133.8 | C-H | $\text{C}_{60} \text{H}_{26}$ | 12.23 (817.5) | 363.0 | C-H |
| | 12.68 (788.4) | 200.4 | C-H | | 12.71 (787.1) | 225.9 | C-C |
| | 12.71 (786.7) | 290.5 | C-C | | 13.28 (753.2) | 50.7 | C-H |
| $\text{C}_{26} \text{H}_{14}^+$ | 11.78 (848.7) | 162.2 | C-H | $\text{C}_{30} \text{H}_{16}^+$ | 12.27 (815.2) | 186.5 | C-H |
| | 12.68 (788.9) | 1.7 | C-C | | 12.68 (788.9) | 6.86 | C-C |
| | 12.73 (785.5) | 20.1 | C-H | | 13.44 (743.8) | 53.36 | C-H |

Frequencies are scaled. Infrared intensities are in km mol^{-1} .